

Supplementary Materials

Novel Tricarbonylrhenium-Anthrapyrazole Complexes with DNA-Binding and Antitumor Properties: In Vitro and In Vivo Pharmacokinetic Studies with ^{99m}Tc -analogue

Georgios Paparidis ¹, Melpomeni Akrivou ², George Psomas ³, Ioannis S. Vizirianakis ^{2,4}, Antonios Hatzidimitriou ³, Catherine Gabriel ^{5,6}, Dimosthenis Sarigiannis ^{5,6} and Dionysia Papagiannopoulou ^{1,*}

¹ Laboratory of Pharmaceutical Chemistry, School of Pharmacy, Faculty of Health Sciences, Aristotle University of Thessaloniki, 54124 Thessaloniki, Greece

² Laboratory of Pharmacology, School of Pharmacy, Faculty of Health Sciences, Aristotle University of Thessaloniki, 54124 Thessaloniki, Greece

³ Department of General and Inorganic Chemistry, Faculty of Chemistry, Aristotle University of Thessaloniki, 54124 Thessaloniki, Greece

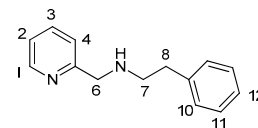
⁴ Department of Health Sciences, School of Life & Health Sciences, University of Nicosia, Nicosia 2417, Cyprus

⁵ Environmental Engineering Laboratory, Department of Chemical Engineering, Aristotle University of Thessaloniki, 54124 Thessaloniki, Greece

⁶ HERACLES Research Center on the Exposome and Health, Center for Interdisciplinary Research and Innovation, Balkan Center, Bldg. B, 10th km Thessaloniki-Thermi Road, 57001 Thessaloniki, Greece

* Correspondence: papagd@pharm.auth.gr

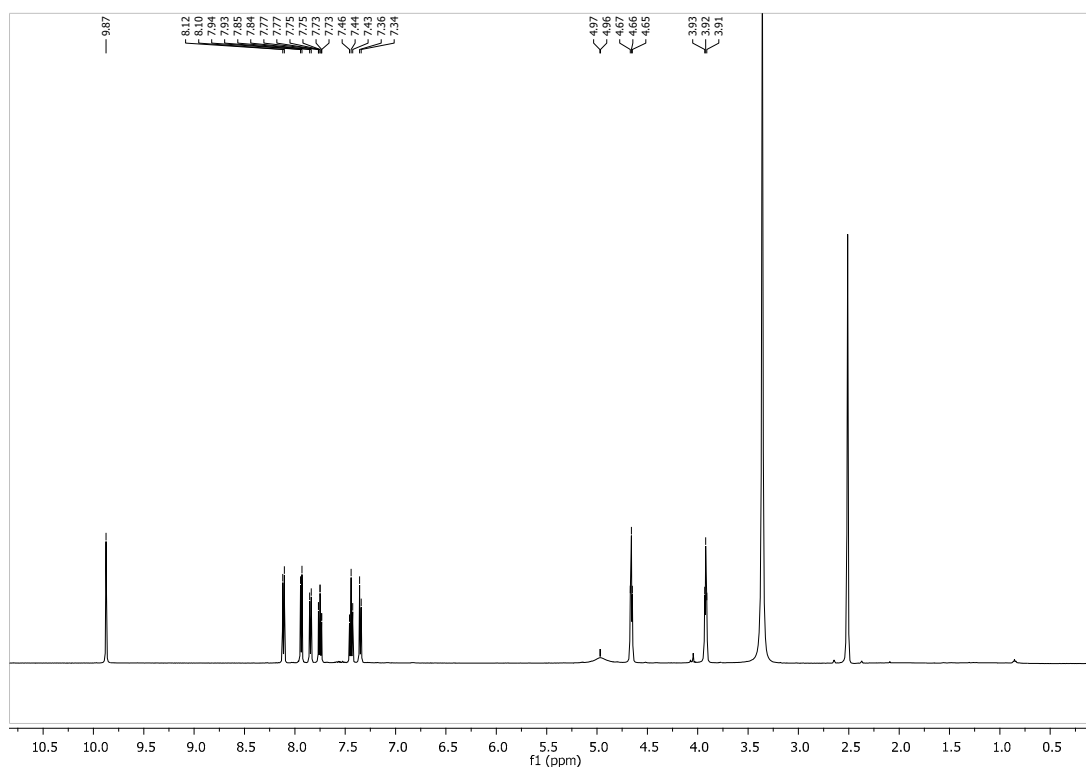
1. Synthesis of 2-phenyl-N-(pyridin-2-ylmethyl)ethanamine (L4)

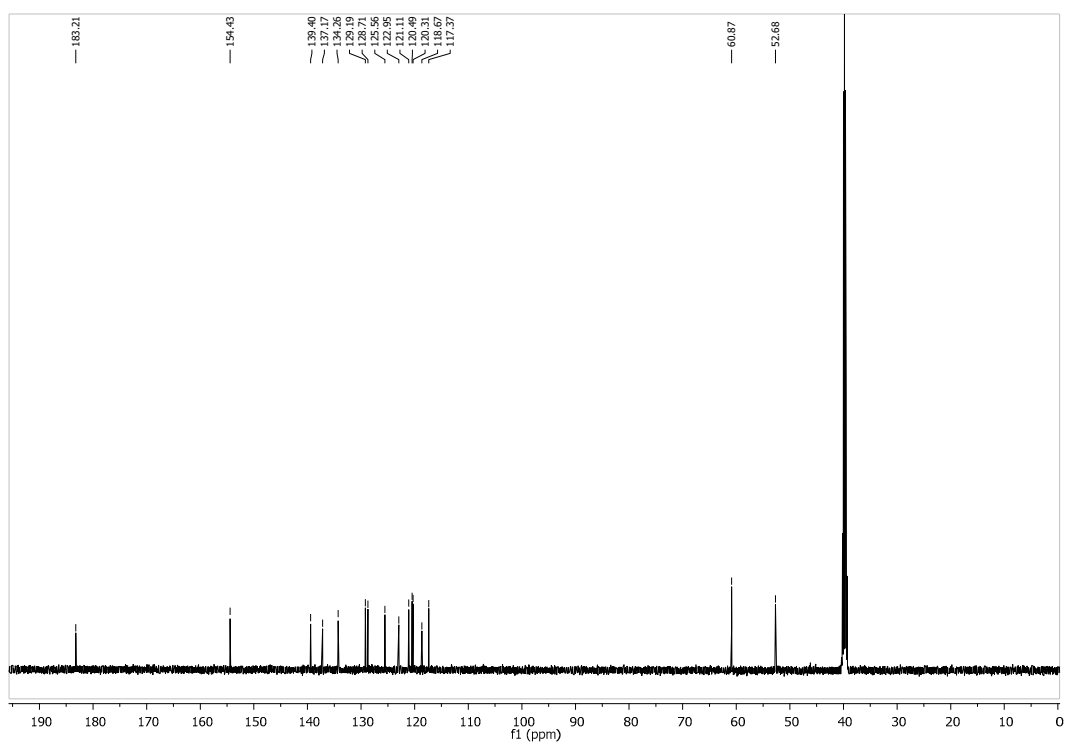


In a 30-mL vial, picolylamine (162 mg, 1.5 mmol), phenethylchloride (141 mg, 1 mmol), anhydrous N,N-dimethylformamide (1mL), potassium carbonate (204 mg, 1.5 mmol) and cat. potassium iodide were added and the vial was crimped and heated at 120 °C for 24 h. Then, the reaction mixture was extracted with brine and dichloromethane (×3) and the organic phase was collected and dried over magnesium sulfate. The filtrate was evaporated to dryness and the product was purified by flash silica gel chromatography (10 g) with ethyl acetate-methanol, 9:1. Yield: 75 mg (35 %). IR (neat, cm^{-1}): 3309, 3056, 3026, 2925, 2854, 1591, 1548. ^1H NMR (500 MHz, CDCl_3 , ppm) δ : 8.53 (d, $J = 4.2$ Hz, H-1, 1H), 7.61 (td, $J = 7.7$, 1.8 Hz, H-3, 1H), 7.32 – 7.24 (m, 3H), 7.20 (d, $J = 7.4$ Hz, 3H), 7.14 (dd, $J = 6.9$, 5.4 Hz, H-2, 1H), 3.99 (s, H-6, 2H), 2.93 (tr, $J = 6.7$ Hz, 2H), 2.85 (tr, $J = 6.9$ Hz, 2H), 2.06 (br, N-H). ^{13}C NMR (126 MHz, CDCl_3 , ppm) δ : 159.69, 149.27, 139.99, 136.45, 128.70, 128.42, 126.11, 122.21, 121.91, 55.15, 50.90, 36.49. ESI-HRMS (m/z): Calc. for $\text{M} = \text{C}_{14}\text{H}_{16}\text{N}_2$: 213.1386 $[\text{M}+\text{H}]^+$; Found: 213.1394 $[\text{M}+\text{H}]^+$.

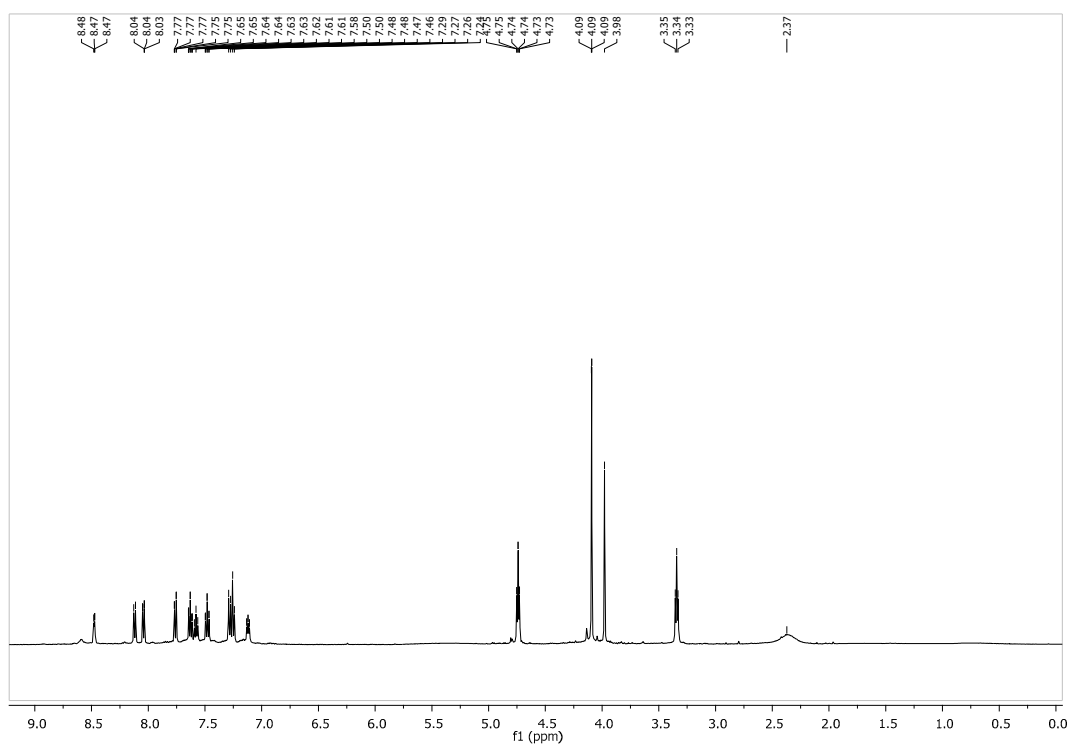
2. NMR spectra

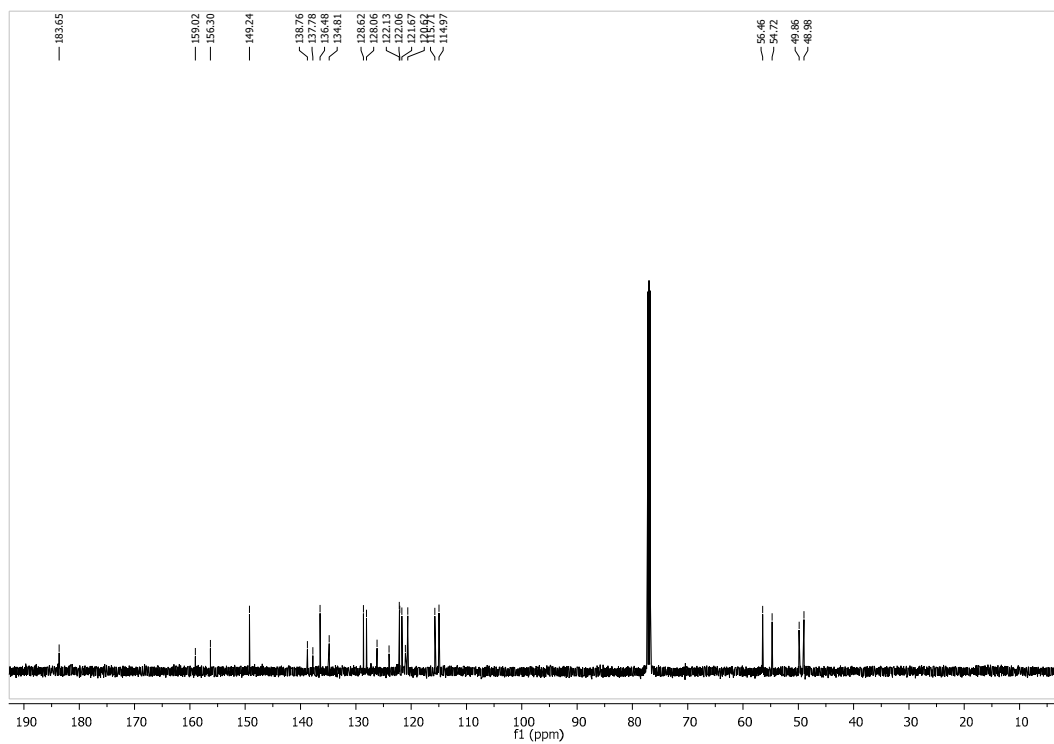
L1



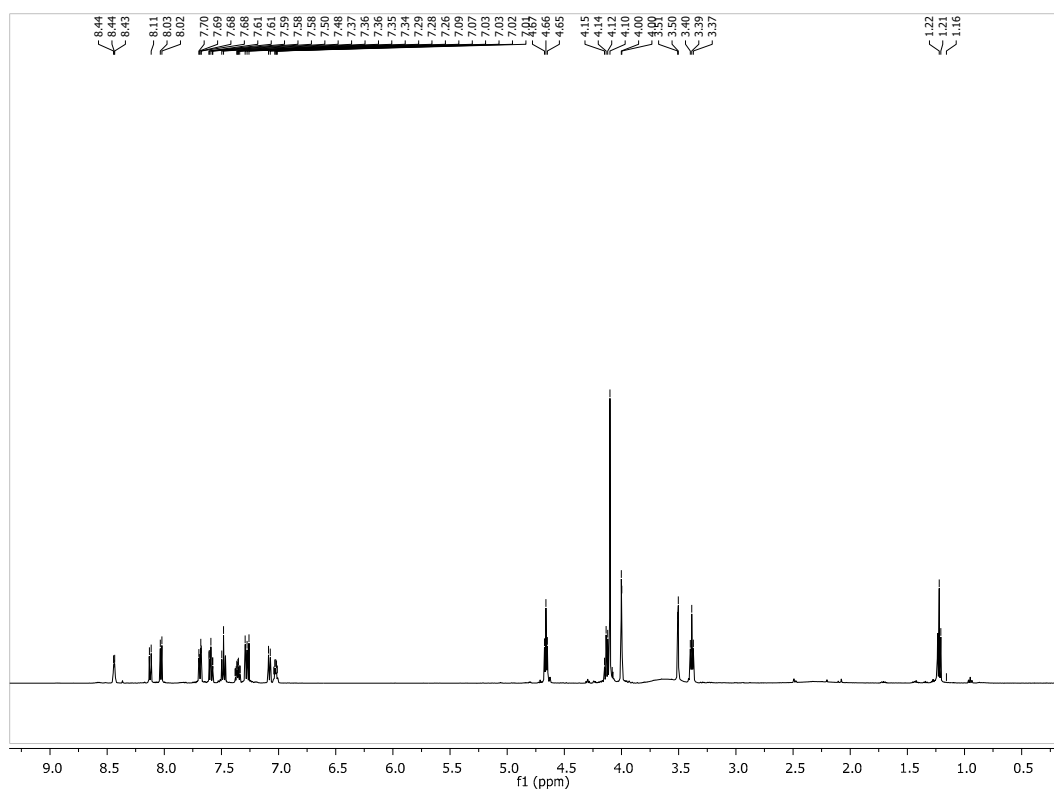


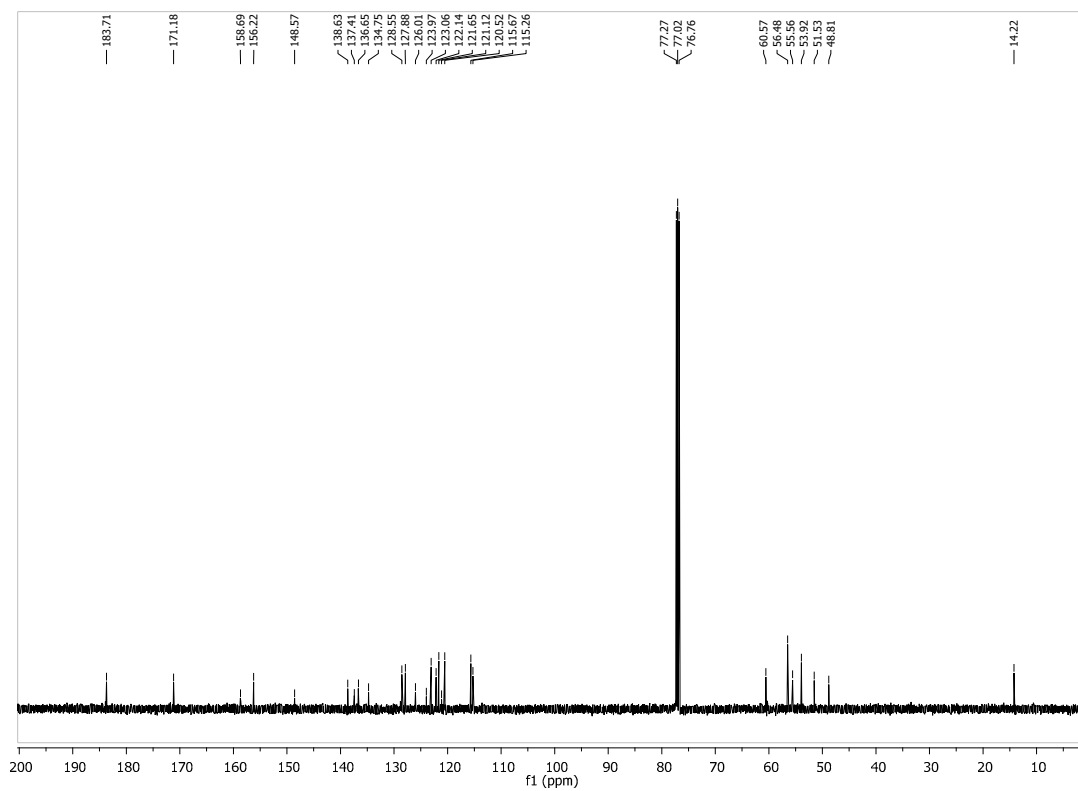
L2



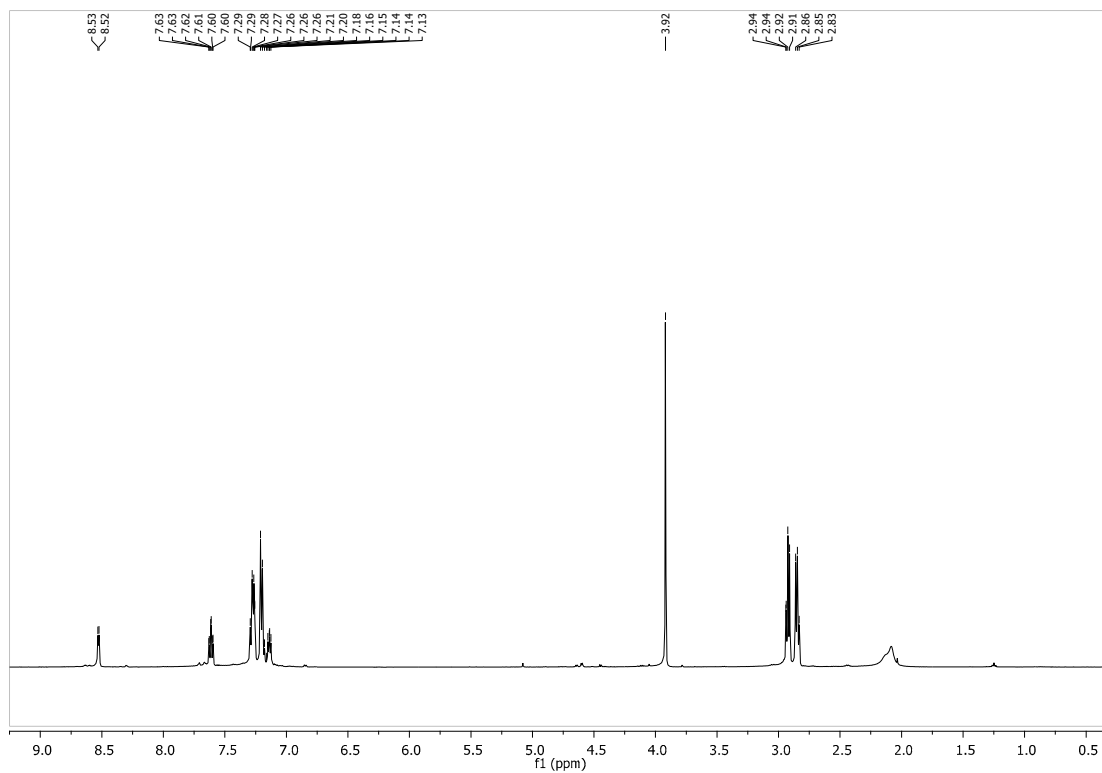


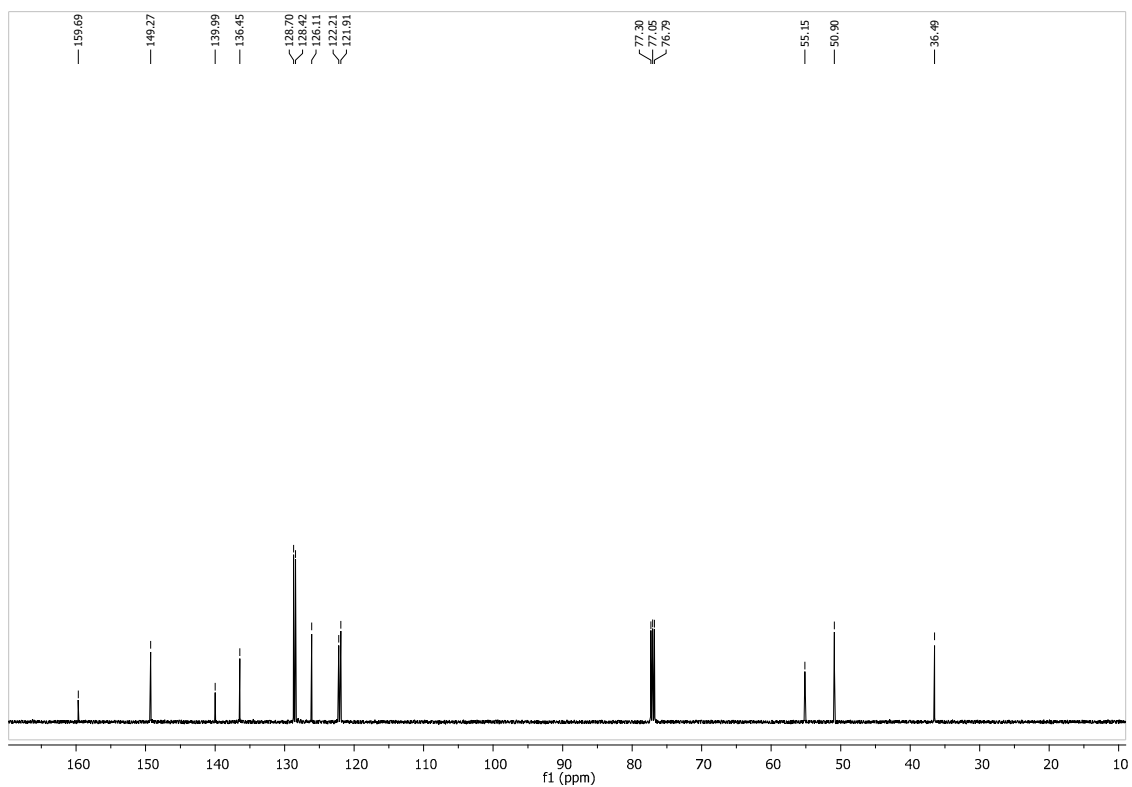
L3



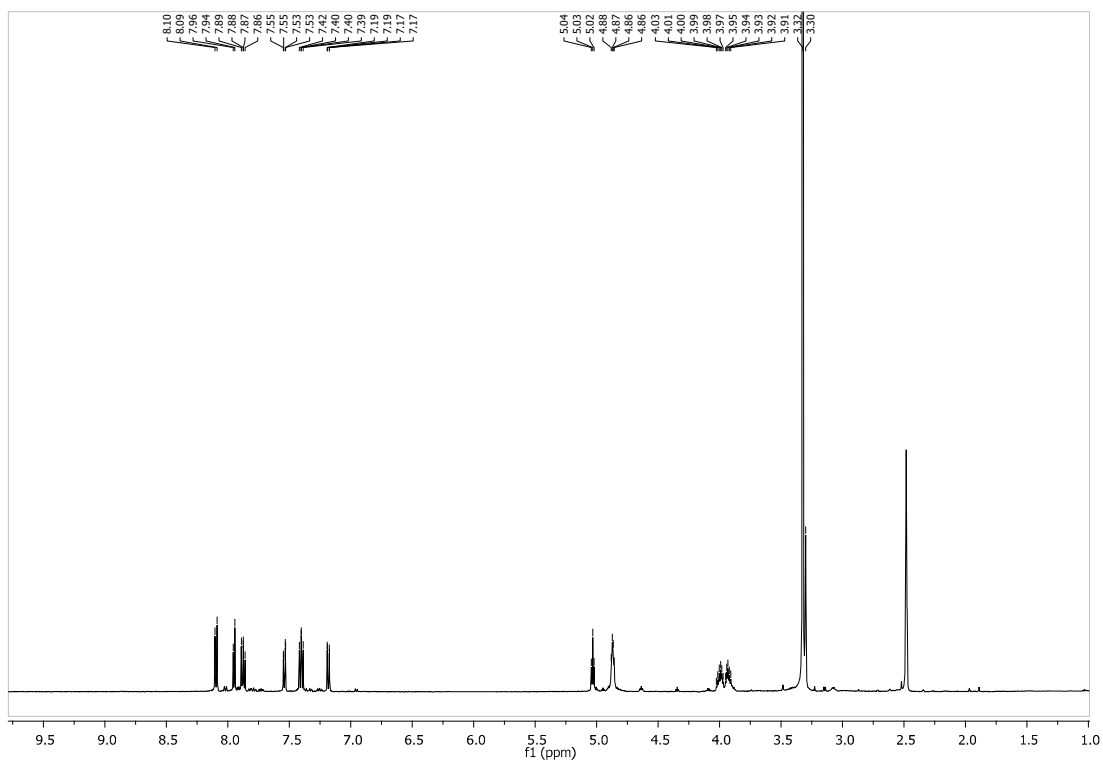


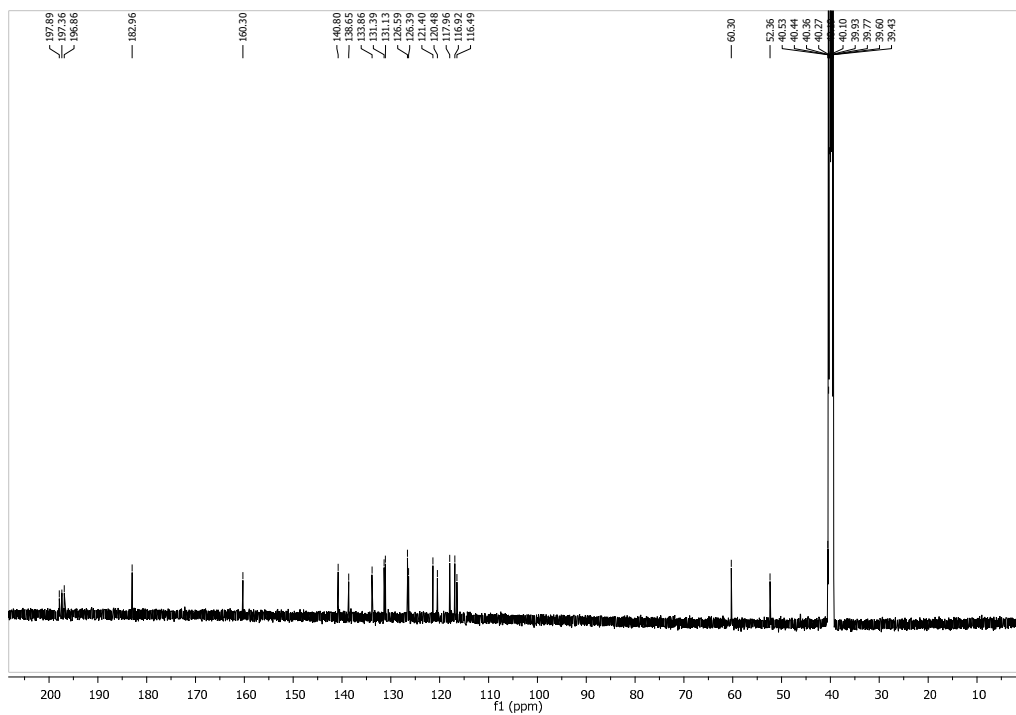
L4



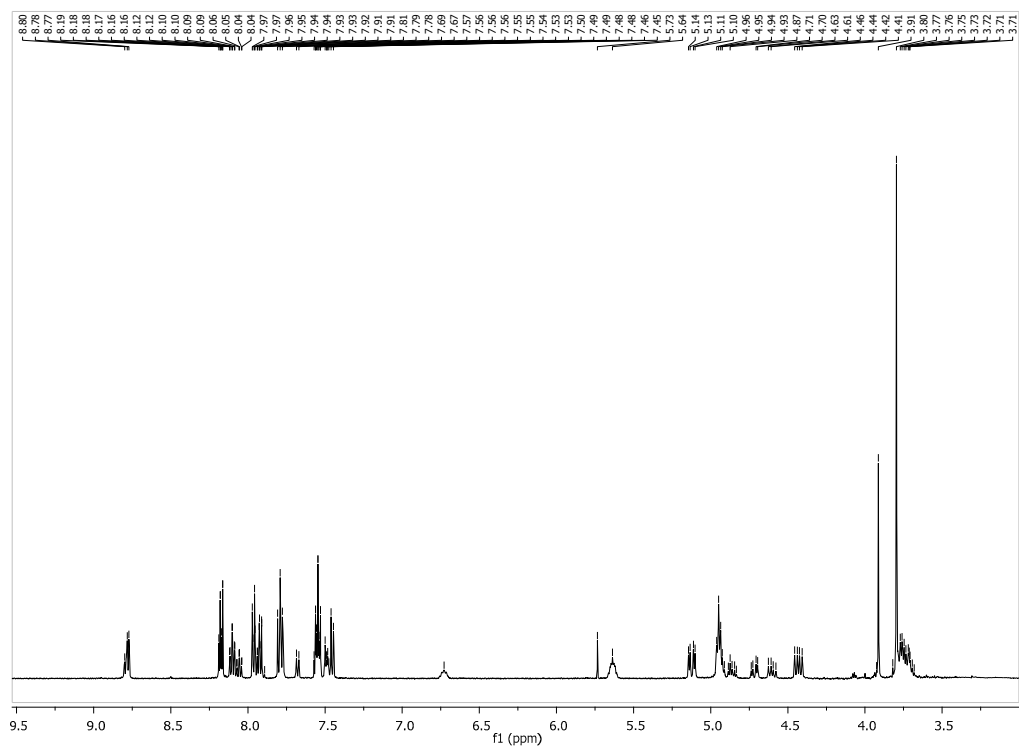


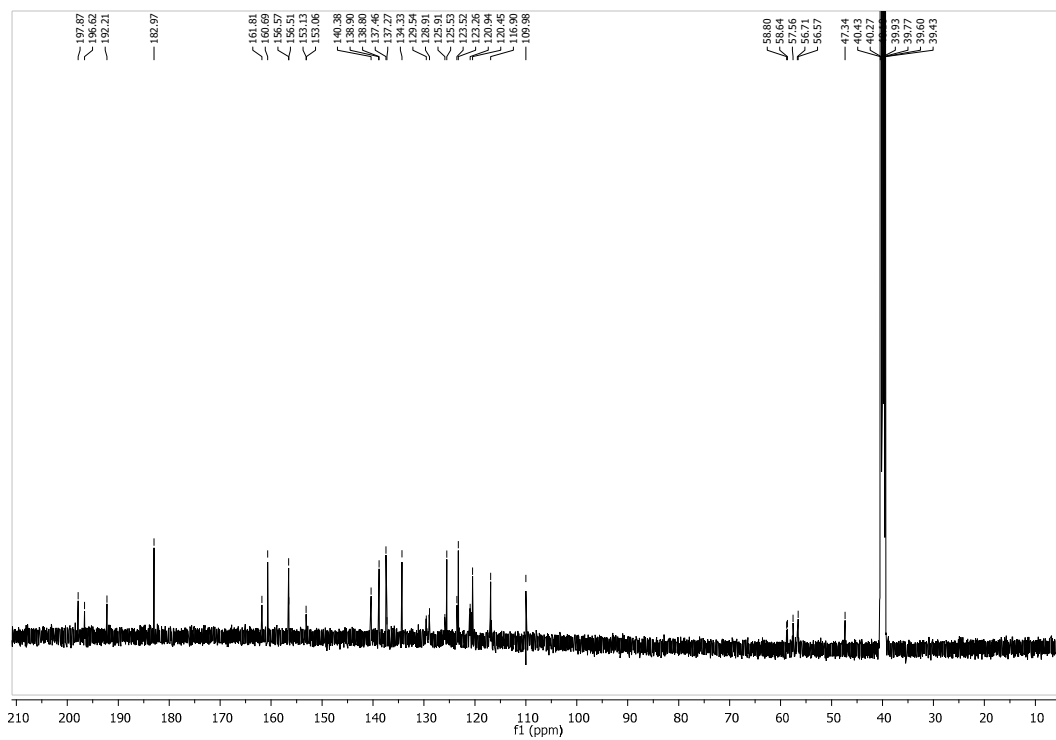
ReL1



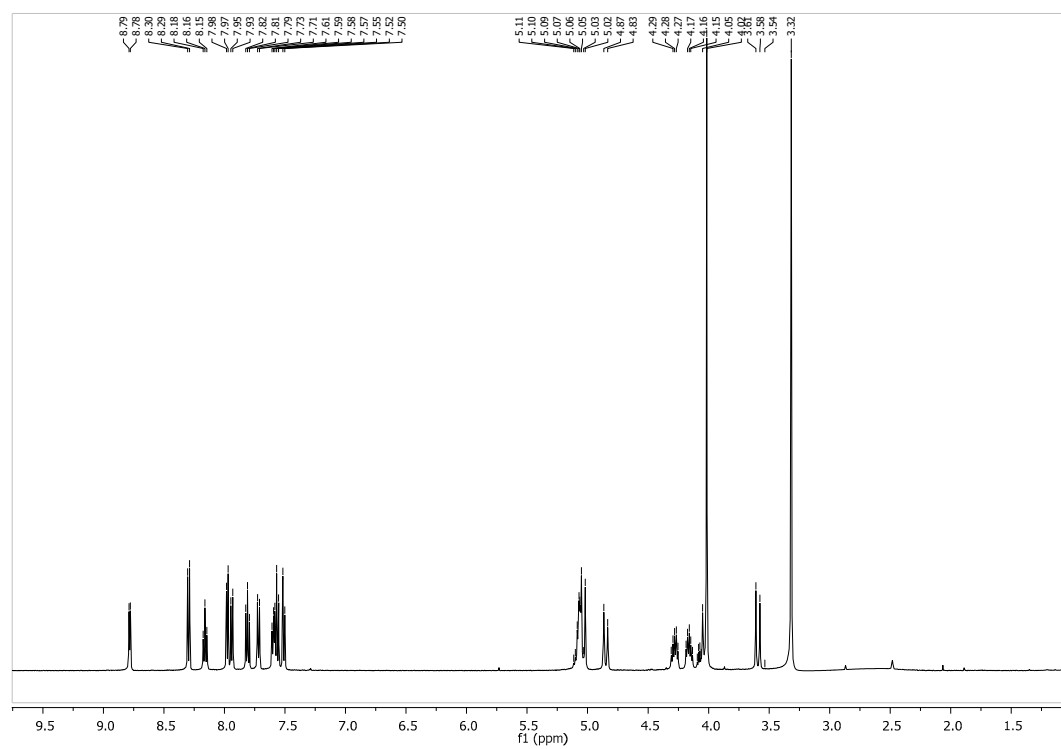


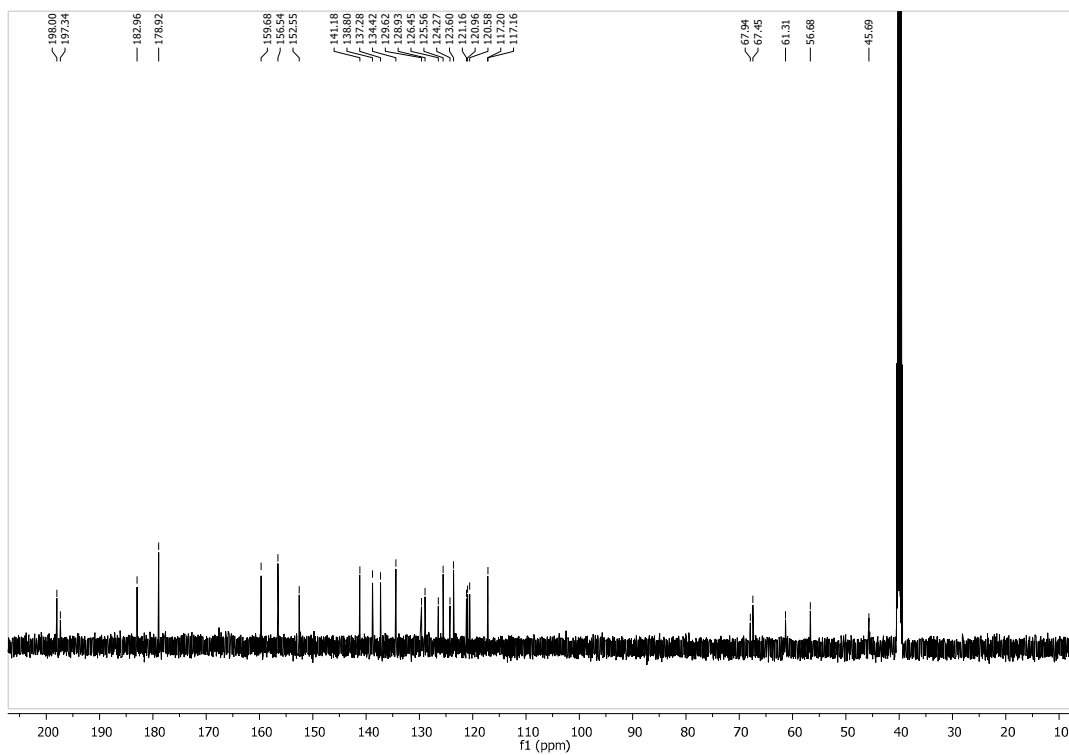
ReL2



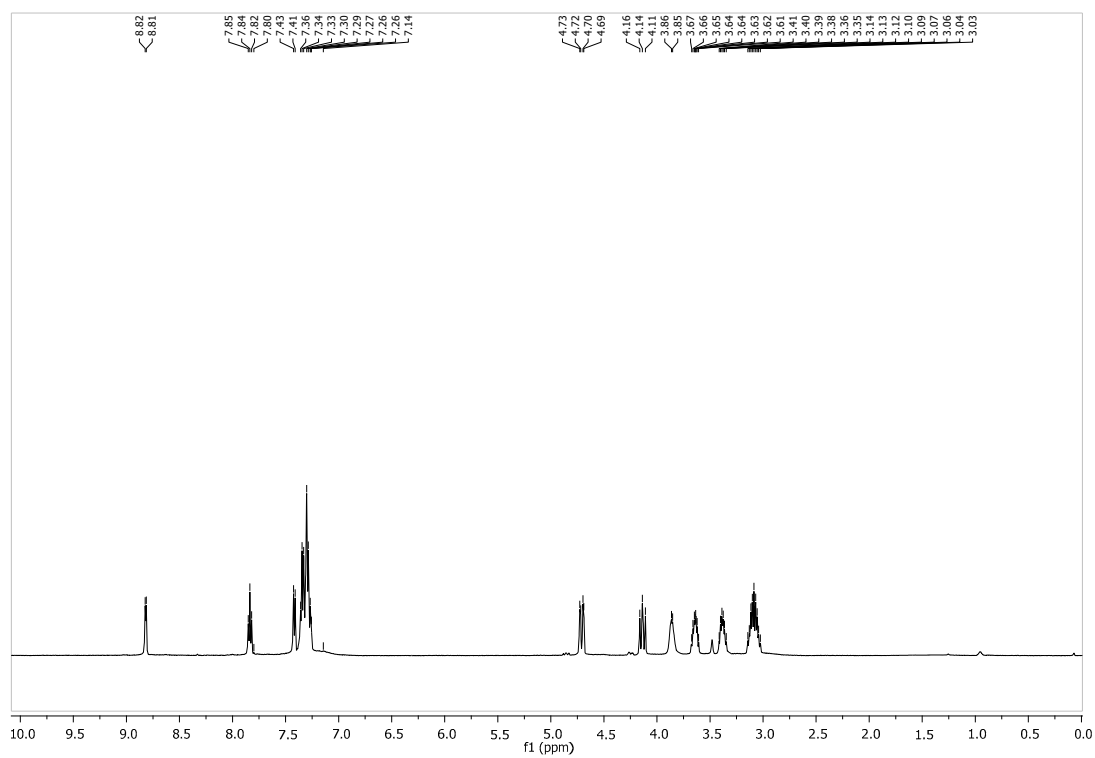


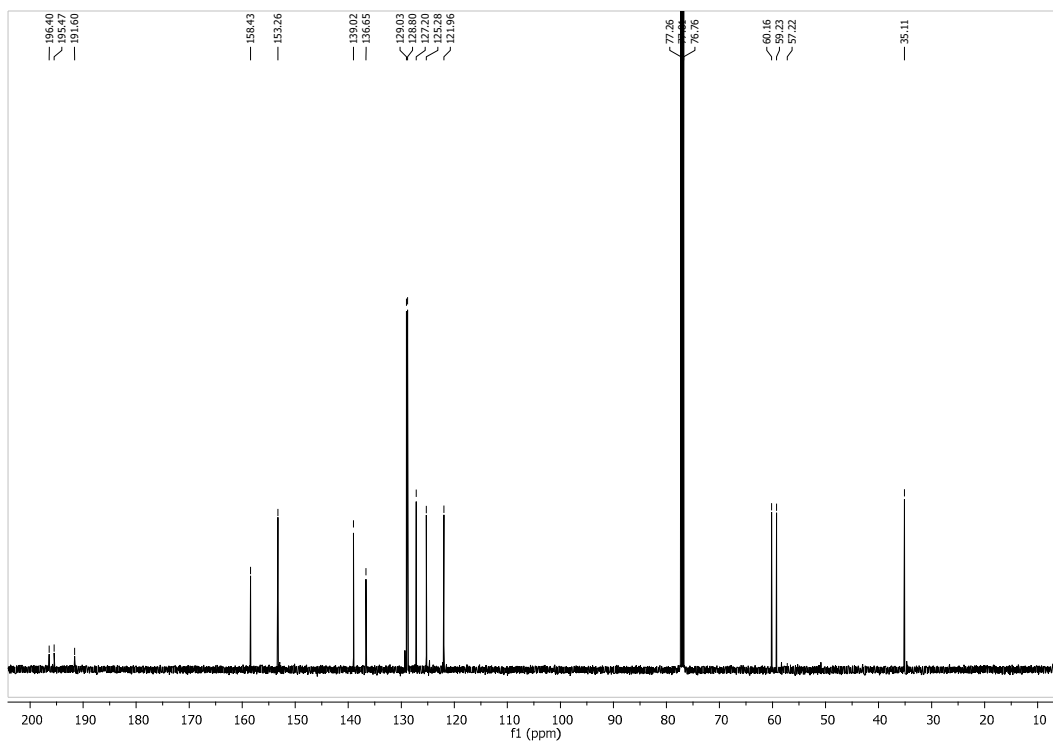
ReL3



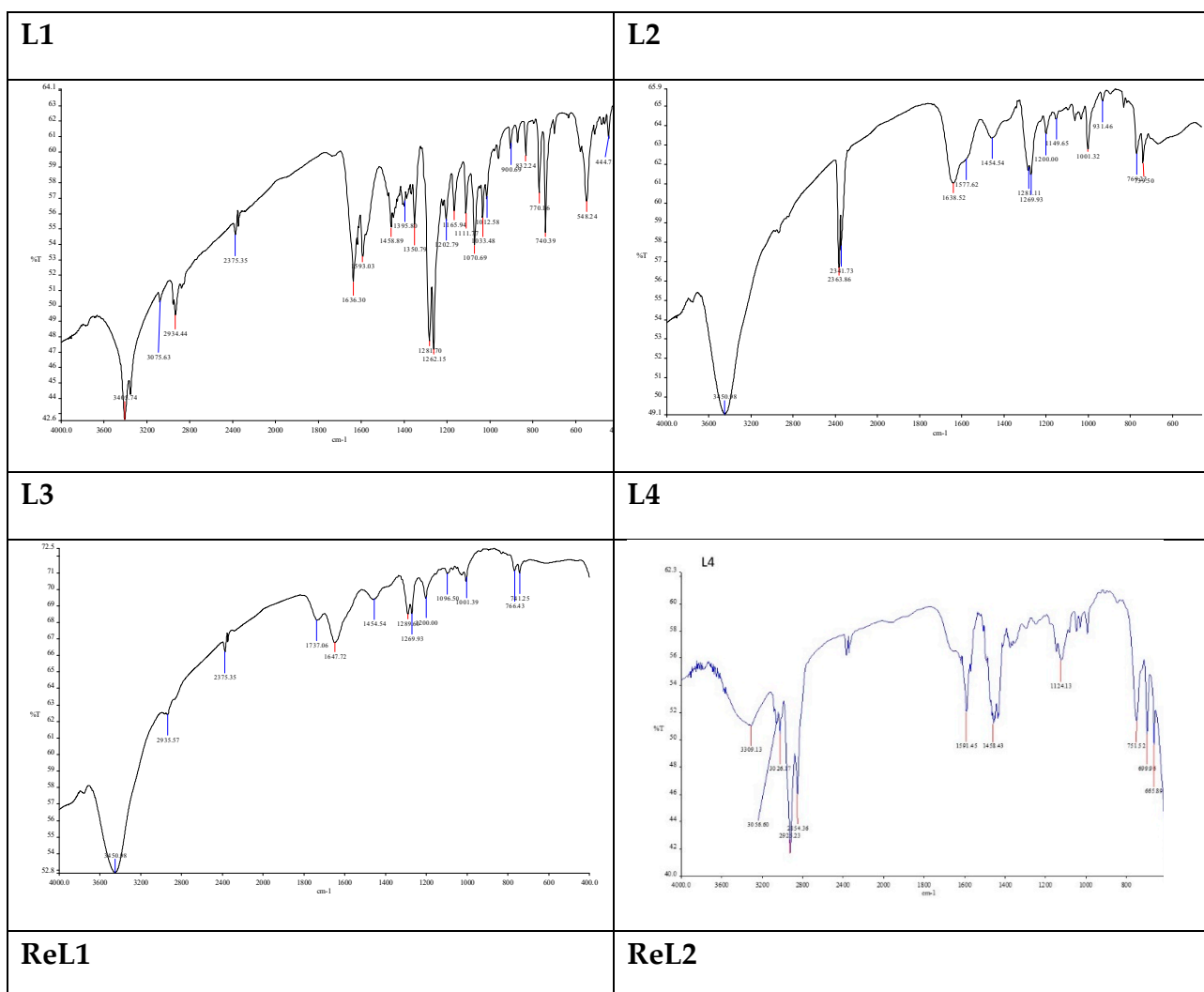


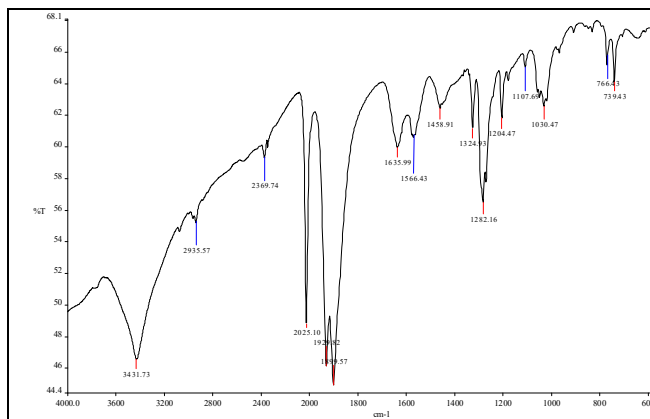
ReL4



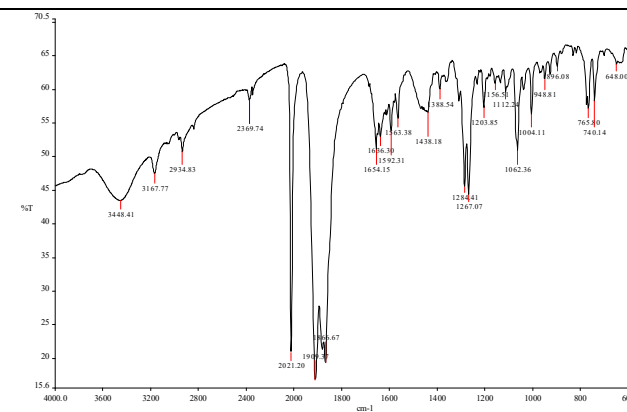
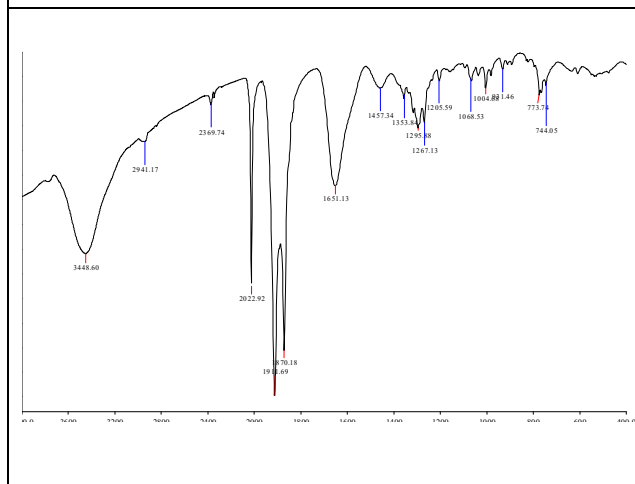


3. IR spectra

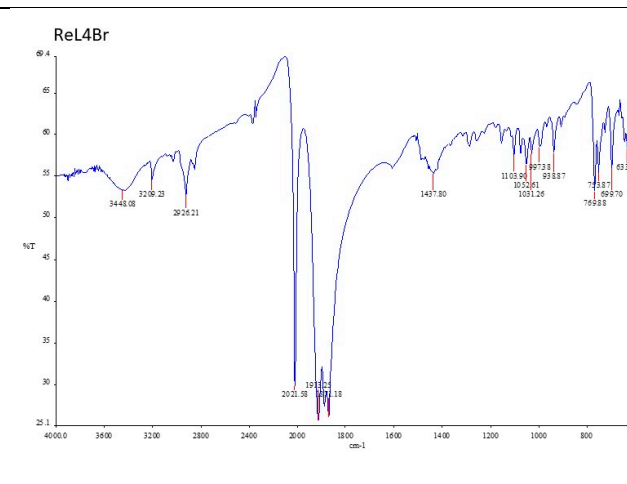




ReL3



ReL4



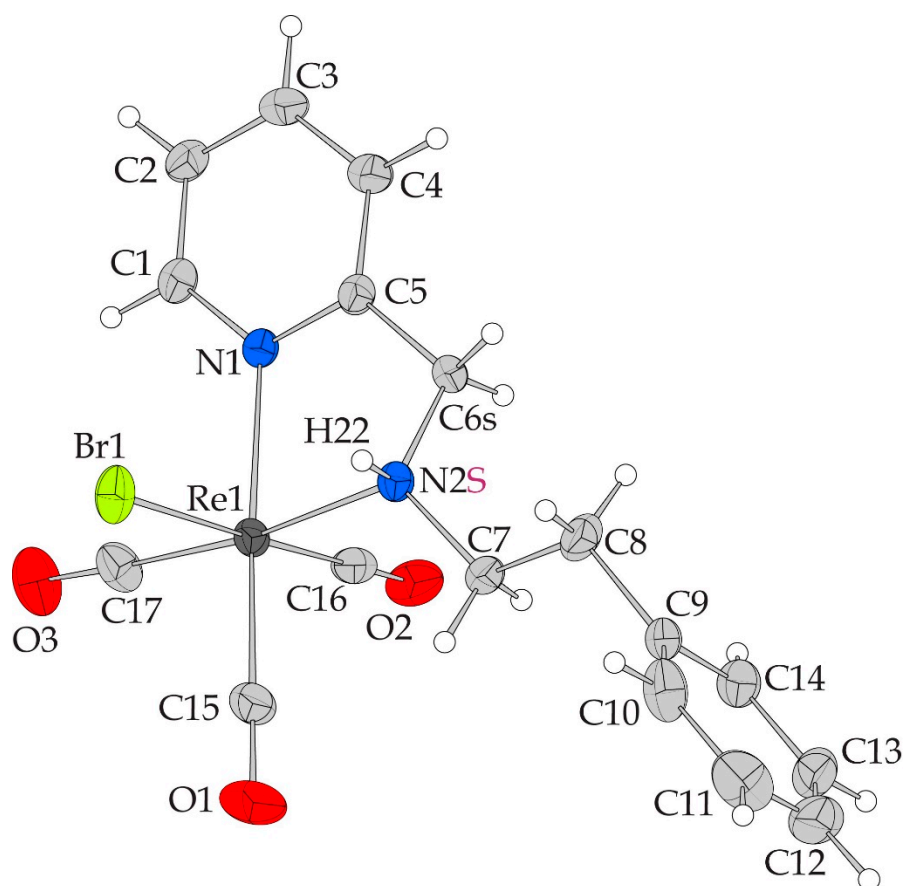


Figure S1. ORTEP diagram of the S enantiomer of **ReL4**.

Table S1. Computed octahedral distortion parameters

Complex	$D_{\text{mean}} (\text{\AA})$	ζ (Zeta) (\AA)	Delta	Σ (Sigma) ($^{\circ}$)	Θ (Theta) ($^{\circ}$)	Volume (\AA^3)
[Re(CO) ₃ Br(L4)]	2.1211	1.306638	0.015025	58.2834	168.1178	12.4500
Complex 9 in [1]	2.1324	1.214425	0.014451	58.7373	162.4430	12.6400
[Re(CO) ₃ Br(L3)] in [2]	2.1209	1.173004	0.013855	59.2341	161.1291	12.4300
[Re(CO) ₃ Br(L3')] in [2]	2.1176	1.210947	0.013937	58.5704	166.0752	12.3600

[1] Wang, W.; Spingler, B.; Alberto, R. *Inorg. Chim. Acta* **2003**, 355, 386–393, doi:<https://doi.org/10.1016/j.ica.2003.08.001>

[2] Song, X.; Lim, M.H.; Mohamed, D.K.B.; Wong, S.M.; Zhao, J.; Hor, T.S.A. *J Organomet. Chem* **2016**, 814, 1–7, doi:<https://doi.org/10.1016/j.jorganchem.2016.04.010>

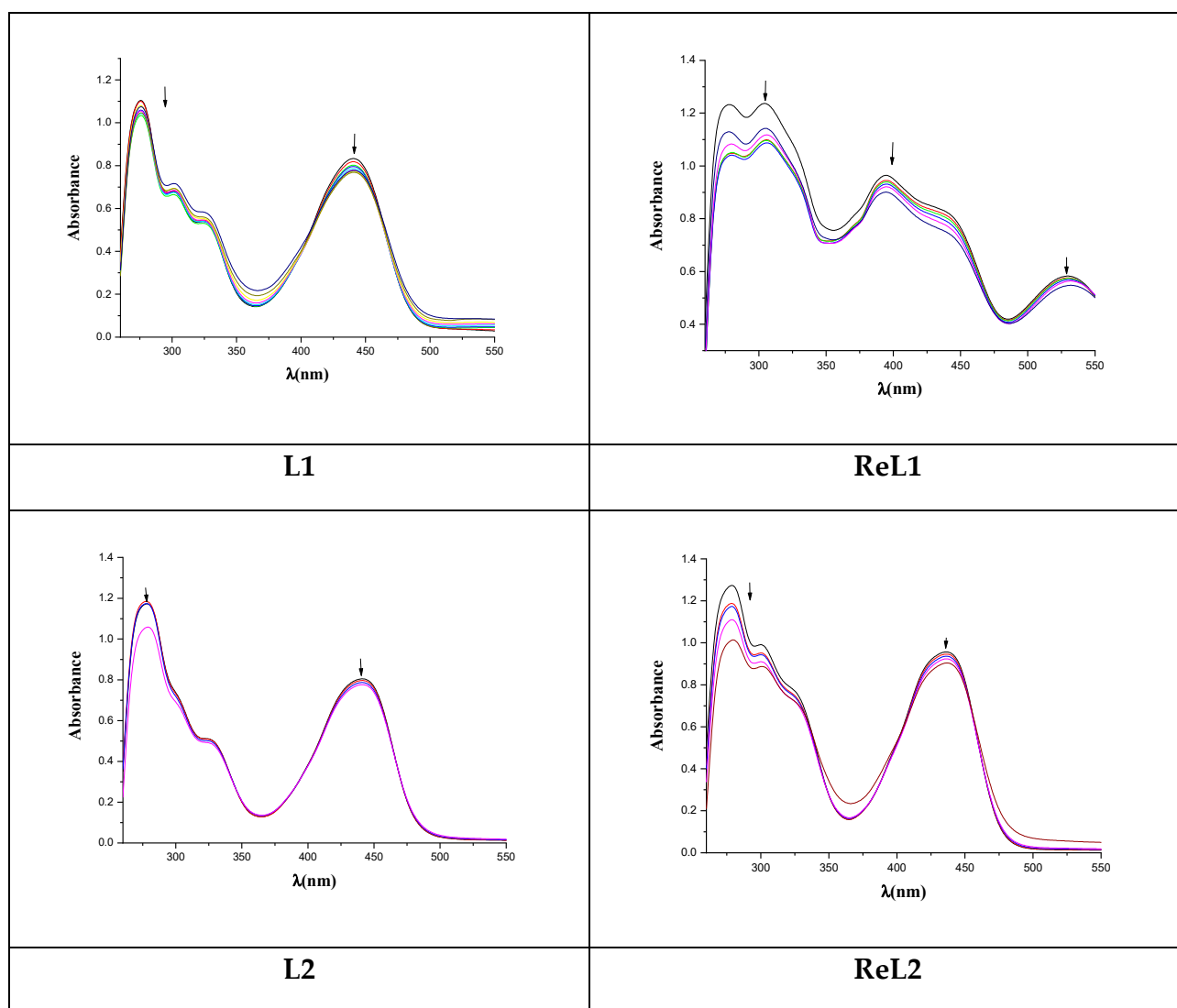


Figure S2. UV-vis spectra of DMSO solution (1×10^{-4} M) of **L1**, **L2**, **ReL1** and **ReL2** in the presence of increasing amounts of CT DNA. The arrows show the changes upon addition of CT DNA.

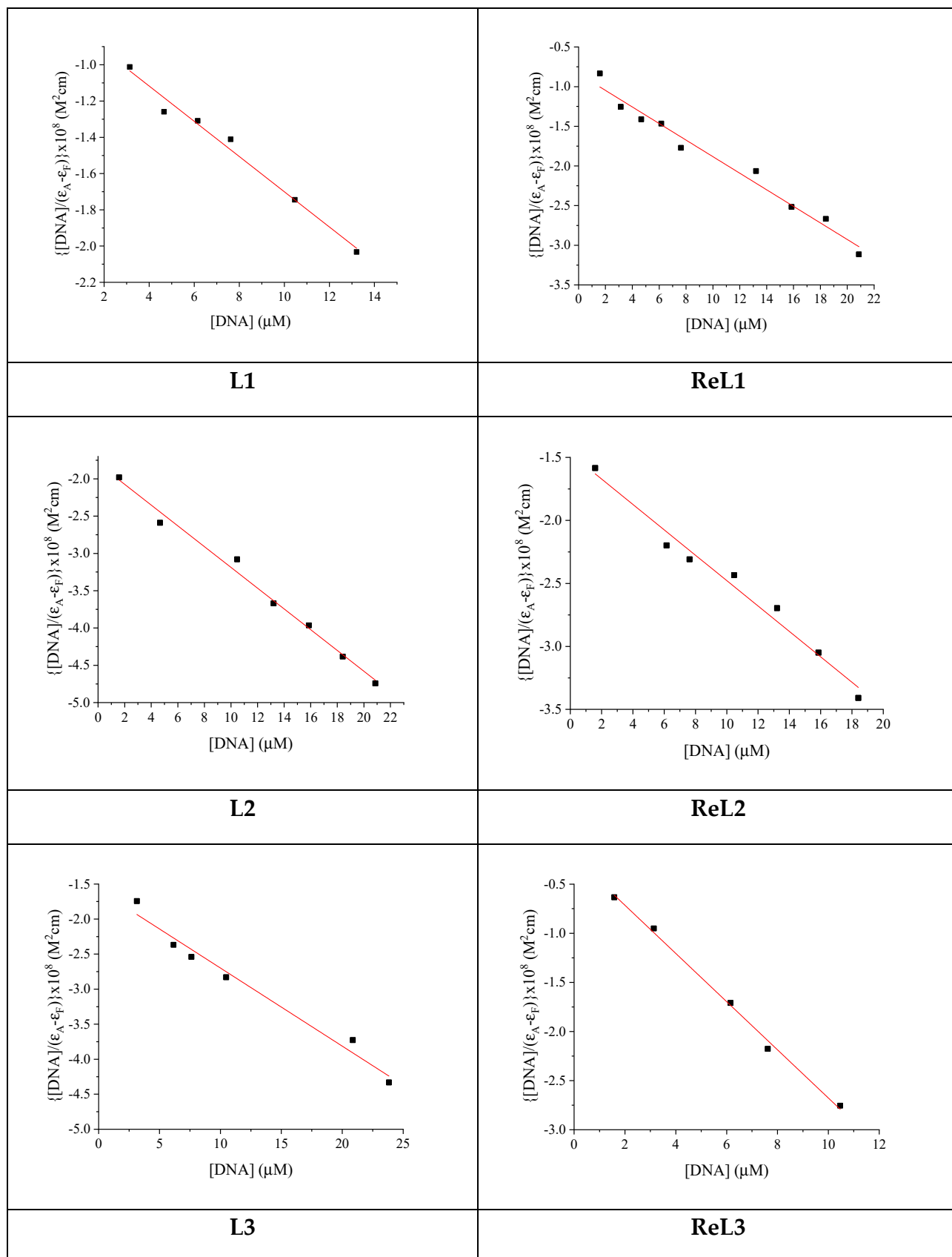


Figure S3. Plot of $\frac{[DNA]}{(\epsilon_A - \epsilon_F)}$ versus $[DNA]$ for compounds **L1–L3** and **ReL1–ReL3**.

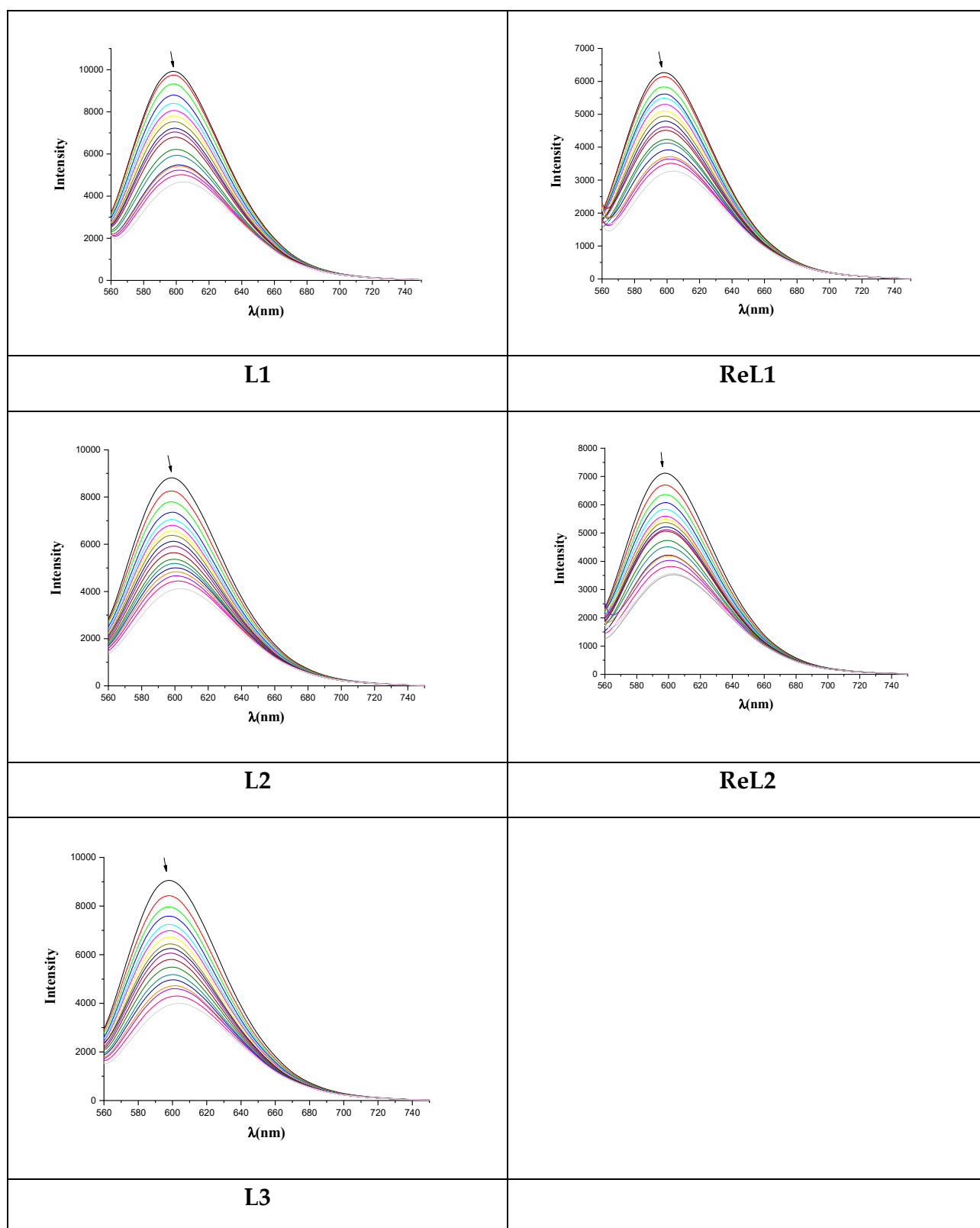


Figure S4. Fluorescence emission spectra ($\lambda_{\text{excitation}} = 540 \text{ nm}$) for EB–DNA ($[\text{EB}] = 20 \mu\text{M}$, $[\text{DNA}] = 26 \mu\text{M}$) in buffer solution in the absence and presence of increasing amounts of compounds **L1-L3** and **ReL1-ReL2** (up to the value of $r = 0.4$). The arrow shows the changes of intensity upon of the compound.

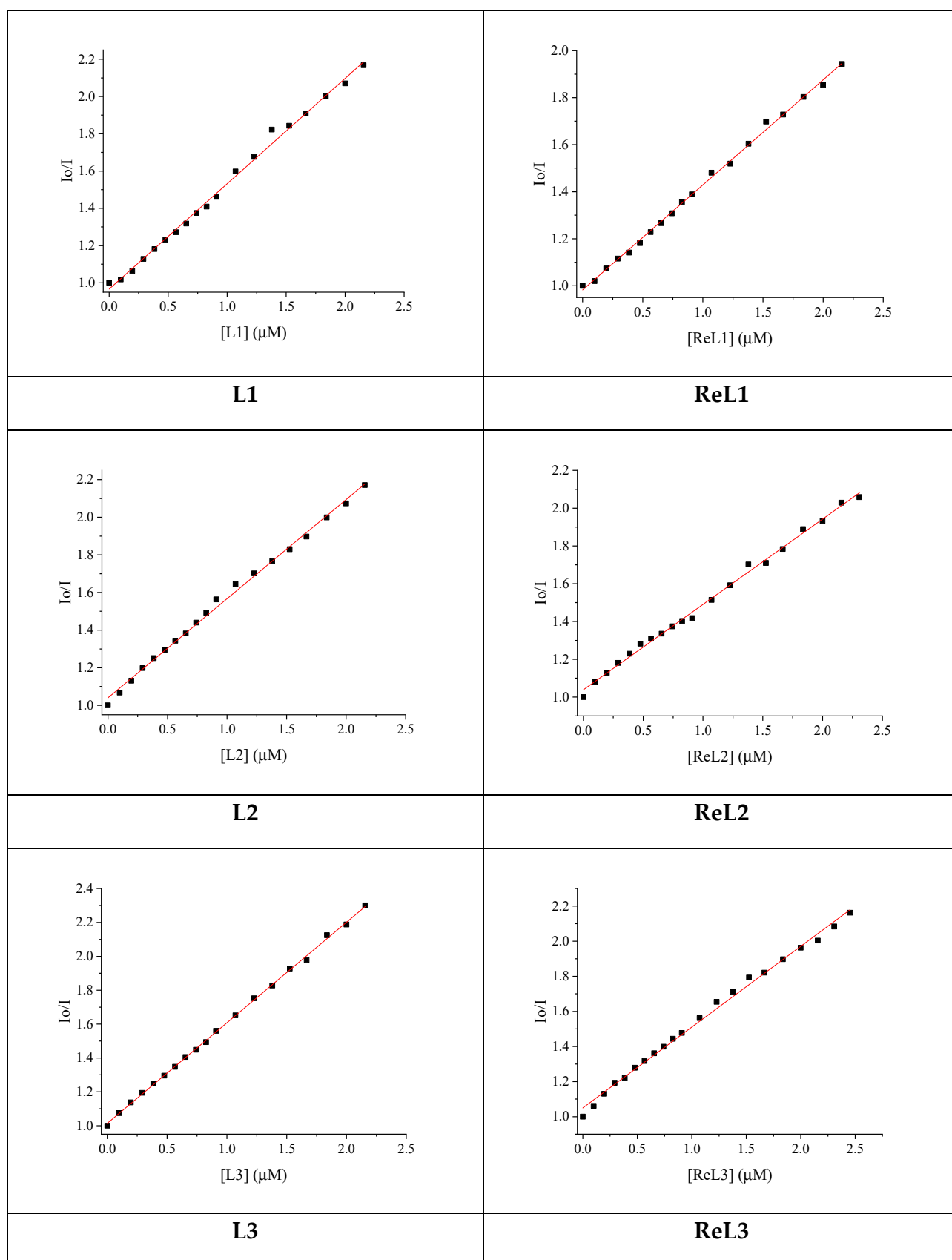


Figure S5. Stern–Volmer quenching plot of EB–DNA fluorescence for compounds **L1–L3** and **ReL1–ReL3**.

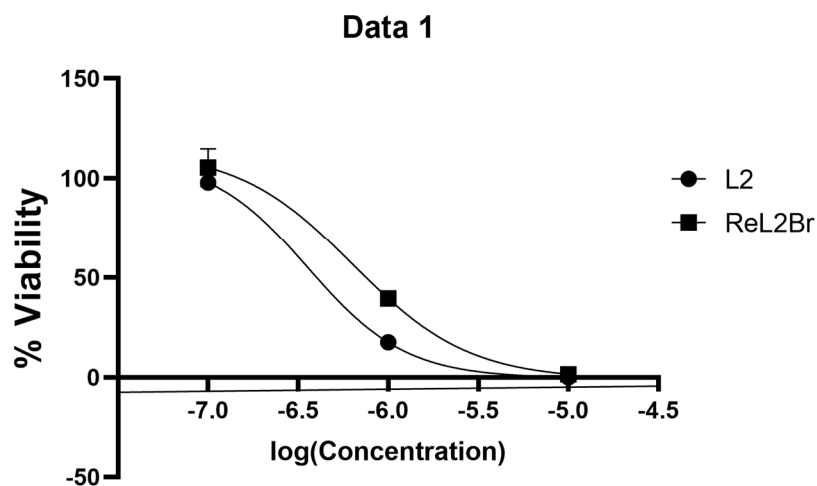


Figure S6. IC₅₀ curve of **L2** and **ReL2**.

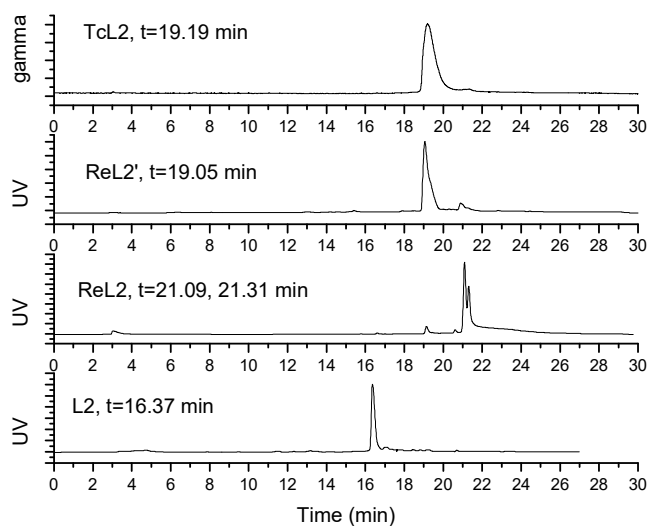


Figure S7. Comparative HPLC analysis of **L2**, $t_R = 16.37$ min, **ReL2**, $t_R = 21.09, 21.31$ min, **ReL2'** [$\text{Re}(\text{CO})_3\text{L2}(\text{MeOH})$] OTf , $t_R = 19.05$ min, and $^{99\text{m}}\text{TcL2}$, $t_R = 19.19$ min.